

Bicyclic 1-Hydroxy-2-oxo-1,2-dihydropyridine-3-carboxamide-Containing HIV-1 Integrase Inhibitors Having High Antiviral Potency against Cells Harboring Raltegravir-Resistant Integrase Mutants

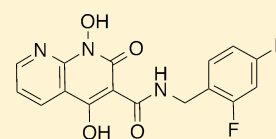
Xue Zhi Zhao,[†] Steven J. Smith,[‡] Mathieu Métifiot,^{§,||} Barry C. Johnson,[‡] Christophe Marchand,[§] Yves Pommier,[§] Stephen H. Hughes,[‡] and Terrence R. Burke, Jr.*[†]

[†]Chemical Biology Laboratory, National Cancer Institute-Frederick, National Institutes of Health, Frederick, Maryland 21702, United States

[‡]HIV Drug Resistance Program, National Cancer Institute-Frederick, National Institutes of Health, Frederick, Maryland 21702, United States

[§]Laboratory of Molecular Pharmacology, Center for Cancer Research, National Cancer Institute, National Institutes of Health, Bethesda, Maryland 20892, United States

ABSTRACT: Integrase (IN) inhibitors are the newest class of antiretroviral agents developed for the treatment of HIV-1 infections. Merck's Raltegravir (RAL) (October 2007) and Gilead's Elvitegravir (EVG) (August 2012), which act as IN strand transfer inhibitors (INSTIs), were the first anti-IN drugs to be approved by the FDA. However, the virus develops resistance to both RAL and EVG, and there is extensive cross-resistance to these two drugs. New "2nd-generation" INSTIs are needed that will have greater efficacy against RAL- and EVG-resistant strains of IN. The FDA has recently approved the first second generation INSTI, GSK's Dolutegravir (DTG) (August 2013). Our current article describes the design, synthesis, and evaluation of a series of 1,8-dihydroxy-2-oxo-1,2-dihydroquinoline-3-carboxamides, 1,4-dihydroxy-2-oxo-1,2-dihydro-1,8-naphthyridine-3-carboxamides, and 1-hydroxy-2-oxo-1,2-dihydro-1,8-naphthyridine-3-carboxamides. This resulted in the identification of noncytotoxic inhibitors that exhibited single digit nanomolar EC₅₀ values against HIV-1 vectors harboring wild-type IN in cell-based assays. Importantly, some of these new inhibitors retain greater antiviral efficacy compared to that of RAL when tested against a panel of IN mutants that included Y143R, N155H, G140S/Q148H, G118R, and E138K/Q148K.



Antiviral Efficacy
 EC₅₀ = 0.006 μM
 SI > 20,000

INTRODUCTION

After 30 years of intensive research, approximately 30 drugs have been approved for the treatment of acquired immunodeficiency syndrome (AIDS).^{1,2} Of these, integrase (IN) inhibitors are the newest drug class² with Merck's Raltegravir (RAL, 1) (October 2007)³ and Gilead's Elvitegravir (EVG, 2) (August 2012)⁴ being the first IN inhibitors to be approved by the FDA (Figure 1). These agents selectively block the strand transfer step (ST) of the integration reaction as compared with the 3'-processing step (3'-P). For this reason, these drugs are called IN strand transfer inhibitors (INSTIs).⁵ INSTIs, including RAL and EVG, share key structural features. These include a coplanar arrangement of three heteroatoms, whose function is to chelate the two catalytically important Mg²⁺ ions at the IN active site, which are held in place by a conserved DDE motif (D64, D116, and E152 in HIV-1 IN).⁶ Additionally, a halobenzyl ring is present that interacts with the penultimate cytosine base near the 3'-end of the viral DNA. This displaces the dA at the very 3'-end of the viral DNA and in so doing prevents the insertion of the viral DNA into the host genome.⁷ Treatment with RAL and EVG can lead to the development of resistance, and there is extensive shared cross-resistance.^{8–10} Therefore, "2nd-generation" INSTIs are being developed that have greater efficacies against RAL and EVG-resistant strains of IN.¹¹ GSK's Dolutegravir (DTG, 3, Figure 1) is a second-

generation INSTI that has recently received FDA approval for the treatment of AIDS.^{1,12,13} However, the finding that DTG, like all anti-HIV drugs, selects for resistant viruses,¹² emphasizes the continuing need to develop INSTIs that can effectively inhibit HIV strains that carry the common/extant resistance mutations.

An attractive property of DTG is its ability to maintain high potencies against mutant strains of HIV that are resistant to RAL and EVG.¹⁴ Although DTG contains key structural features that are found in other INSTIs (outlined above and highlighted in Figure 1), it differs in having its halobenzyl group appended via an amide carbonyl that is proximal to but not part of the triad of metal chelating heteroatoms. This is in contrast to RAL and several other INSTIs, in which the halobenzyl amide carbonyl serves as one of the metal-chelating elements in the heteroatom triad. As a result, the halobenzyl linker moiety of DTG has greater flexibility than RAL structurally related INSTIs. This flexibility may contribute to DTG's ability to bind tightly to both wild-type (WT) and mutant IN–DNA complexes.^{15–18} While differing in their halobenzyl linker arrangements, both RAL and DTG have a hydroxyl group as the central component of their metal-chelating triad of

Received: December 11, 2013

Published: January 28, 2014

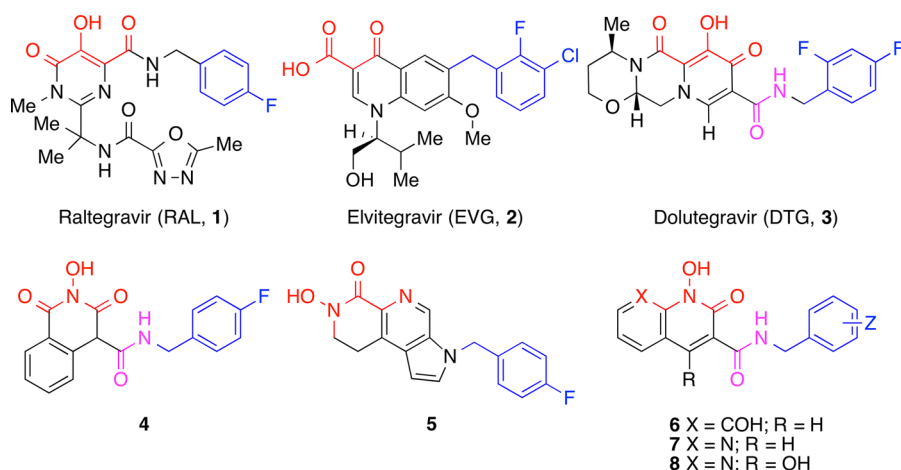


Figure 1. Structures of HIV-1 integrase inhibitors discussed in the text. Mg^{2+} -chelating heteroatoms are shown in red with the halogen-substituted aromatic functionality shown in blue. The amide linkers are shown in magenta.

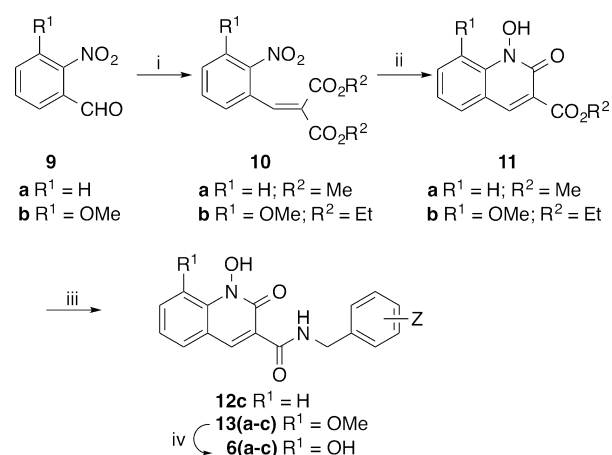
heteroatoms. We noted that hydroxyl amides can function as high affinity metal-chelating groups.¹⁹ In fact, hydroxylamide-containing INSTIs (for example **4**) have been reported, which combine a centrally located hydroxylamide metal chelating functionality with flexible halobenzylamide group like the one in DTG.^{20–24} Alternatively, inhibitors such as **5** employ a hydroxylamide group as the terminal member of the metal-chelating triad, and the halobenzyl group is appended through a 1*H*-pyrrole ring (Figure 1).²⁵ Our current report describes new INSTIs (**6–8**, Figure 1) that have a hydroxylamide group as the central component of a triad of metal-chelating heteroatoms, which originate from within bicyclic frameworks. Importantly, the halobenzylamide moieties of many of these inhibitors are appended in a fashion that may not require participation of their amide carbonyls in metal chelation. These inhibitors exhibit high potencies against viral vectors that carry WT IN and the major RAL-resistant IN mutants.

RESULTS AND DISCUSSION

Inhibitor Design. In designing the current series of inhibitors, we examined two classes of bicyclic platforms that differed in their presentation of the “left” terminal member of the metal-chelating heteroatom triad. Both of these platforms utilized a 1-hydroxypyridin-2(1*H*)-one moiety as the central and “right” members of the heteroatom triad. However, one class of inhibitor utilized a phenolic hydroxyl as the “left” terminal metal-chelating heteroatom [1,8-dihydroxyquinolin-2(1*H*)-ones **6**], while the second class employed a ring-embedded nitrogen to give 1-hydroxy-1,8-naphthyridine-2(1*H*)-ones (**7**). The latter class of inhibitors was also varied by the introduction of a 4-hydroxyl substituent [1,4-dihydroxy-1,8-naphthyridine-2(1*H*)-ones **8**] (Figure 1). Three different halogen-substituted benzylamides were examined at the 3-position of the “right” 1-hydroxypyridin-2(1*H*)-one ring because the nature and pattern of halogen phenyl substitution is known to significantly affect the IN inhibitory potency of INSTIs.²⁶

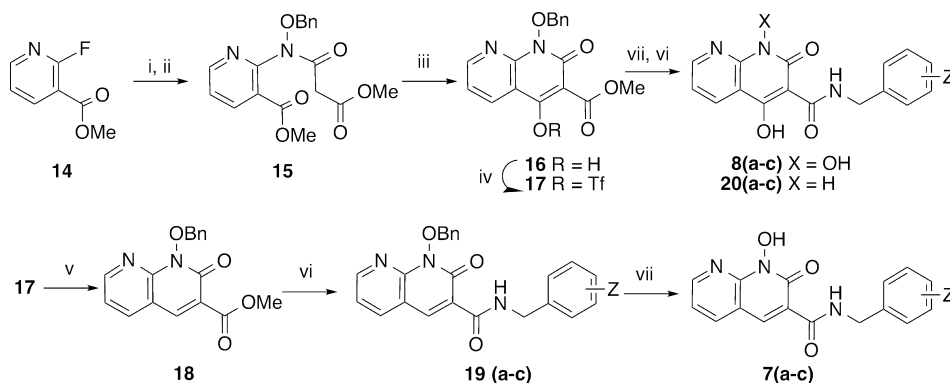
Synthesis. Modification of a previously reported²⁷ low-yield Knoevenagel condensation of *o*-nitrobenzaldehyde **9a** with diethyl malonate using microwave radiation and a solvent mixture that included benzene provided dimethyl 2-(2-nitrobenzylidene)malonate **10a** in quantitative yield (Scheme 1).²⁸ Treatment of 3-methoxy-2-nitrobenzaldehyde **9b** with

Scheme 1. Synthesis of Analogues **6a–c** and **12c**^a



^aReagents and conditions: (i) HOAc (4 equiv), $\text{CH}_2(\text{CO}_2\text{Me})_2$ or $\text{CH}_2(\text{CO}_2\text{Et})_2$ (12 equiv), piperidine (1.2 equiv), microwave, 80 °C; (ii) H_2 , PtO₂ (0.15 equiv), rt; (iii) 3-Cl-4-F-BnNH₂ (a), 3,4-diF-BnNH₂ (b) or 2,4-diF-BnNH₂ (c), 60 °C; iv) BBr_3 , CH_2Cl_2 , rt.

diethyl malonate under similar conditions but without the inclusion of benzene gave the corresponding diethyl 2-(3-methoxy-2-nitrobenzylidene)malonate **10b** in 90% yield. Initial hydrogenation of **10a** (0.15 equiv of platinum(IV) oxide) using previously reported conditions that did not contain DMSO,²⁷ provided a very low yield of the desired methyl 1-hydroxy-2-oxo-1,2-dihydroquinoline-3-carboxylate **11a**, accompanied by significant reduction of the C3–C4 double bond and the *N*-hydroxyl group. However, when the reduction was performed on **10b** with the inclusion of DMSO (1.6 equiv),^{29,30} the desired ethyl 1-hydroxy-8-methoxy-2-oxo-1,2-dihydroquinoline-3-carboxylate **11b** was obtained in 82% yield. In choosing the composition and pattern of halogen substitution on the benzyl amide group, we selected 3'-chloro-4'-fluorobenzyl **13a** and 3',4'-difluorobenzyl **13b**, respectively, based on our previous findings that these can provide improved IN inhibitory potencies.^{26,31} In addition, we prepared the 2',4'-difluorobenzyl-substituted pattern **12c** and **13c** found in DTG. Demethylation of **13a–c** with boron tribromide gave the desired final products 1,8-dihydroxy-2-oxo-1,2-dihydroquinoline-3-carboxamides, **6a–c** (Scheme 1).

Scheme 2. Synthesis of Analogues 7a–c and 8a–c and Over-reduced Products 20a–c^a

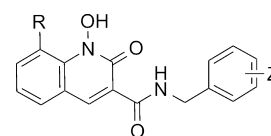
^aReagents and conditions: (i) BnONH₂, DMSO, 140 °C; (ii) ClCOCH₂CO₂CH₃, NEt₃, CH₂Cl₂, rt; (iii) NaOMe, MeOH, rt; (iv) Tf₂O, 0 °C; (v) PdCl₂(PPh₃)₂, TIS, NEt₃, 85 °C; (vi) (a) 3-Cl-4-F-BnNH₂, (b) 3,4-diF-BnNH₂, or (c) 2,4-diF-BnNH₂; (vii) H₂, Pd-C.

Because DTG is unsubstituted at the position para to its central metal-chelating hydroxyl group (the 2-position of its 5-hydroxy-4-oxo-1,3-dihydropyridine-3-carboxamide moiety), we prepared a series of 1-hydroxy-2-oxo-1,2-dihydro-1,8-naphthyridine-3-carboxamides (7), which lack a substituent at the corresponding position. Accordingly, in a fashion similar to reported methodology,³² treatment of commercially available methyl 2-fluoronicotinate **14** with benzoxylamine in DMSO followed by acylation of the resulting methyl 2-((benzyloxy)-amino)nicotinate with methyl 3-chloro-3-oxopropanoate gave the intermediate methyl 2-(*N*-(benzyloxy)-3-methoxy-3-oxopropanamido)nicotinate **15** (Scheme 2). This was treated with sodium methoxide in methanol to yield the cyclized product, methyl 1-(benzyloxy)-4-hydroxy-2-oxo-1,2-dihydro-1,8-naphthyridine-3-carboxylate **16** (66% yield for three steps from **14**) (Scheme 2). Removal of the 4-hydroxy group was achieved by conversion of **16** to its triflate **17** followed by reduction, and the resulting methyl 1-(benzyloxy)-2-oxo-1,2-dihydro-1,8-naphthyridine-3-carboxylate **18** was reacted individually with neat 3-chloro-4-fluorobenzylamine (a), 3,4-difluorobenzylamine (b) and 2,4-difluorobenzylamine (c) to provide the corresponding amides **19a–c** (Scheme 2). Finally, hydrogenolytic deprotection of the *N*-hydroxyl group gave the desired 1-hydroxy-2-oxo-1,2-dihydro-1,8-naphthyridine-3-carboxamides, (**7a–c**) (Scheme 2). Alternatively, debenzoylation of **16** followed by treatment with halobenzylamines (a, b, and c) in DMF afforded the desired 1,4-dihydroxy-2-oxo-1,2-dihydro-1,8-naphthyridine-3-carboxamides (**20a–c**) (Scheme 2).

Evaluation in *in Vitro* IN Biochemical Assays.

Compounds were evaluated in an IN biochemical assay using radiolabeled oligonucleotides to measure the ability of the compounds to inhibit the 3'-P and ST reactions.³³ For the 1,8-dihydroxyquinolin-2(1*H*)-ones (**6**), 3'-P reactions were inhibited with IC₅₀ values in the micromolar range, with the 3'-Cl-4'-F and 3',4'-diF-substituted amides (**6a**, 3'-P IC₅₀ = 17 μM; and **6b**, 3'-P IC₅₀ = 24 μM) being slightly more potent than the 2',4'-disubstituted analogue **6c** (3'-P IC₅₀ = 43 μM) (Table 1). These results are consistent with our previous reports that among the diverse halogen substituent patterns we tested, 3-chloro-4-fluoro benzylamides show the best potencies in *in vitro* assays.^{26,31} Selectivity for the ST reaction relative to the 3'-P reaction is a defining characteristic of INSTIs, and in the case of **6a** and **6b**, selectivity was approximately 30-fold (ST

Table 1. Inhibitory Potencies of 1,8-Dihydroxy-2-oxo-1,2-dihydroquinoline-3-carboxamides 6(a–c) and 1-Hydroxy-2-oxo-1,2-dihydroquinoline-3-carboxamides 12c and 13c Using an *in Vitro* IN Assay

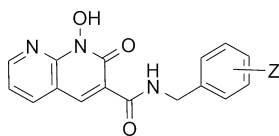


no.	R	Z	IC ₅₀ values (μM)	
			3'-processing	strand transfer
6a	OH	3'-Cl-4'-F	17 ± 1	0.53 ± 0.13
6b	OH	3', 4'-diF	24 ± 3	0.78 ± 0.22
6c	OH	2', 4'-diF	43 ± 5	18 ± 7
12c	H	2', 4'-diF	>333	19.7 ± 2.7
13c	OCH ₃	2', 4'-diF	>333	>333

IC₅₀ values of 0.53 μM and 0.78 μM, respectively; Table 1). In contrast, for **6c** the ST inhibitory potency (ST IC₅₀ = 18 μM) was very similar to its 3'-P inhibitory potency. There was approximately a 20-fold loss of ST inhibitory potency in going from the 3',4'-diF to the 2',4'-diF benzylamide substituent pattern. With the latter pattern of halogen substituents, removal of the 8-hydroxy group abrogated 3'-P inhibitory potency (**12c**, 3'-P IC₅₀ >333 μM) but had little effect on ST inhibitory potency (**12c** ST IC₅₀ = 19.7 μM). Insertion of a bulky methoxyl group at the 8-position (**13c**) also abrogated both 3'-P and ST inhibitory potencies (Table 1).

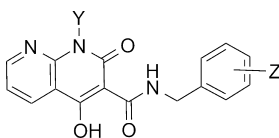
Using the *in vitro* IN catalytic assay described above, we showed that compounds **7a** and **7b** exhibited potent ST inhibition, with IC₅₀ values (14 nM and 17 nM, respectively, Table 2). These were approximately 40-fold lower than the IC₅₀ values measured for the corresponding 8-dihydroxyquinolin-2(1*H*)-ones (**6a** and **6b**, respectively, Table 1); however, high selectivity for inhibiting the ST reaction versus the 3'-P reaction was maintained. Unexpectedly, compound **7c**, which contains the benzyl 2',4'-diF pattern found with DTG, while being slightly less potent (2-fold) than either the 3'-Cl-4'-F or 3',4'-diF containing compounds (**7a** and **7b**, respectively), exhibited a greater than 400-fold enhancement of ST inhibitory potency (IC₅₀ ≈ 40 nM) relative to the corresponding 8-dihydroxyquinolin-2(1*H*)-one (**6c**).

Given the potentially important role of the carboxamide linker arrangement in DTG's ability to maintain efficacy against

Table 2. Inhibitory Potencies of 1-Hydroxy-2-oxo-1,2-dihydro-1,8-naphthyridine-3-carboxamides 7(a–c) Using an *in Vitro* IN Assay

no.	Z	IC ₅₀ values (μM)	
		3'-processing	strand transfer
7a	3'-Cl-4'-F	9.4 ± 1.5	0.014 ± 0.003
7b	3', 4'-diF	13.6 ± 1.8	0.017 ± 0.003
7c	2', 4'-diF	6.1 ± 0.8	0.041 ± 0.012

RAL- and EVG-resistant strains of mutant IN,^{15–17} we inserted a hydroxyl group at the 4-position of the 1-hydroxy-1,8-naphthyridine-2(1H)-one ring system to ask whether this could potentially influence the inhibitory profiles by hydrogen bonding with the 3-carboxamide carbonyl. However, this modification resulted in a slight loss of ST inhibitory potencies (8a–c, Table 3). We also showed that removing the

Table 3. Inhibitory Potencies of 1,4-Dihydroxy-2-oxo-1,2-dihydro-1,8-naphthyridine-3-carboxamides 8(a–c) and 4-Dihydroxy-2-oxo-1,2-dihydro-1,8-naphthyridine-3-carboxamides 20(a–c) Using an *in Vitro* IN Assay

no.	Y	Z	IC ₅₀ values (μM)	
			3'-processing	strand transfer
8a	OH	3'-Cl-4'-F	4.7 ± 0.7	0.027 ± 0.006
8b	OH	3', 4'-diF	3.6 ± 0.6	0.040 ± 0.010
8c	OH	2', 4'-diF	1.2 ± 0.2	0.055 ± 0.008
20a	H	3'-Cl-4'-F	125 ± 15	7.8 ± 1.1
20b	H	3', 4'-diF	93 ± 8	8.1 ± 1.8
20c	H	2', 4'-diF	>333	7.1 ± 1.8

hydroxylamide group resulted in a more than two-orders of magnitude loss of ST inhibitory potency (20a–c, Table 3). This is consistent with the important role this hydroxyl may play as the central component of the metal-chelating triad.

Table 4. Antiviral Potencies of Compounds 7(a–c) and 8(a–c) in Cells Infected with HIV-1 Vectors Containing Wild-Type (WT) or Mutant IN

no.	CC ₅₀ (μM) ^a	EC ₅₀ (nM) WT ^b	EC ₅₀ (nM, IN mutants ^c)			SI ^d
			Y143R	N155H	G140S/Q148H	
1	>100	4 ± 2	162 ± 16	154 ± 33	1900 ± 300	>25,000
7a	>250	38 ± 15	34 ± 6	90 ± 6	N/A ^e	>6,579
7b	>250	62 ± 14	40 ± 13	2200 ± 61	N/A ^e	>4,032
7c	>250	5.1 ± 1.9	4.9 ± 0.8	134 ± 23	438 ± 121	>49,020
8a	102 ± 18	35 ± 12	54 ± 9	148 ± 8	489 ± 62	2,914
8b	192 ± 19	20 ± 6	45 ± 12	189 ± 70	507 ± 125	9,600
8c	137 ± 20	6.2 ± 2.9	11 ± 2	31 ± 8	308 ± 125	22,097

^aCytotoxic concentration resulting in 50% reduction in the level of ATP in human osteosarcoma (HOS) cells. ^bValues obtained from cells infected with the lentiviral vector harboring WT IN. ^cCells were infected with viral vectors carrying IN mutations and indicated values in EC₅₀. ^dSelectivity index calculated as the ratio of CC₅₀ to EC₅₀. ^eNot available.

Evaluation of the Compounds in Cell-Based Antiviral Assays.

A primary objective in developing second-generation IN inhibitors is to overcome mutations that are associated with resistance to first-generation inhibitors, such as RAL. To determine the abilities of our current inhibitors to retain efficacy against resistant variants, we evaluated the antiviral potencies in cells infected with one-round HIV-1 vectors that carry mutations that cause resistance to RAL (Table 4).^{10,34,35} In these assays, RAL (1) exhibited an EC₅₀ value (effective concentration resulting in 50% reduction of luciferase reporter signal) of 4 nM in cells infected with virus containing WT IN. Cells infected with viruses containing either the Y143R or the N155H mutant forms of IN, showed significantly elevated EC₅₀ values (162 nM and 154 nM, respectively). An even greater loss of efficacy (EC₅₀ = 1900 nM) was observed with viruses containing the G140S/Q148H double mutant form of IN (Table 4). In similar assays, treatment of WT-infected cells with inhibitors 7a–c and 8a–c gave EC₅₀ values in the low nanomolar range, with analogues 7c and 8c having the 2',4'-diF substituted benzyl group (EC₅₀ values of 5 nM and 6 nM, respectively) showing greater efficacy by several fold relative to analogues having either 3'-Cl-4'-F (7a and 8a) or 3',4'-diF (7b and 8b) substituted benzyl groups. This is in contrast to *in vitro* assays, where analogues bearing the 2',4'-diF-substituted benzyl group were slightly less effective ST inhibition (Tables 2 and 3).

An important feature of the new inhibitors is their ability to maintain high efficacies against RAL-resistant strains. For example, compound 7c exhibits single digit nanomolar antiviral potencies against both WT and the Y143R mutant, while showing a lower potency against the G140S/Q148H mutant (EC₅₀ = 438 nM). However, it is much improved when compared to RAL (1) (EC₅₀ = 1900 nM). Compound 8c also retains good efficacy against the Y143R mutant (EC₅₀ = 11 nM) as well as both the N155H mutant (EC₅₀ = 31 nM; RAL has EC₅₀ = 154 nM) and the G140S/Q148H mutant (EC₅₀ = 308 nM) (Table 4).

While showing nanomolar EC₅₀ values against cells infected with HIV-1 vectors carrying WT and efficacy against some RAL-resistant mutants, analogues 7a–c exhibited very little cytotoxicity, with CC₅₀ values (cytotoxic concentrations were measured as the level of the compound that reduced cellular ATP levels by 50%) greater than 250 μM. In particular, for the 2',4'-difluorobenzyl amide 7c with an EC₅₀ value of 5.1 nM against WT, this gives a selectivity index (SI = CC₅₀/EC₅₀) greater than 49,000 (Table 4). Analogues 8a–c showed CC₅₀

Table 5. Fold Change (FC) of Amides 7c and 8c Compared with That of RAL (1) in Cells Infected with HIV-1 Constructs Carrying WT or Mutant IN

no.	EC ₅₀ (nM) WT ^a	EC ₅₀ (FC, IN mutants ^b)				
		Y143R	N155H	G140S/Q148H	G118R	E138K/Q148K
1	4 ± 2	41×	38×	475×	9×	375×
7c	5.1 ± 1.9	1×	26×	86×	N/A ^c	N/A ^c
8c	6.2 ± 2.9	2×	5×	50×	6×	32×

^aValues obtained from cells infected with a lentiviral vector harboring WT IN. ^bCells were infected with viral constructs carrying IN mutations, and the indicated values correspond to the fold-change (FC) in EC₅₀ relative to WT. ^cNot available.

values between approximately 100 μM (**8a**) and 200 μM (**8b**). In the case of **8c**, which showed a WT EC₅₀ value of 6.2 nM, a SI value greater than 20,000 was achieved.

Because compounds **7c** and **8c** show antiviral potencies similar to those of RAL (**1**) against HIV-1 vectors carrying WT IN, it is important to compare the relative effectiveness of our inhibitors against mutant strains of IN in terms of fold-loss relative to WT. Table 5 contains data showing the efficacy of compounds against the G118R and E138K/Q148K mutants, which have recently been identified through *in vitro* selection studies with second-generation inhibitors.³⁶ Of particular note is the ability of **8c** to maintain efficacy equivalent to that of RAL against the G118R mutant while showing approximately one order of magnitude greater efficacy than RAL against the remaining mutants in the table.

CONCLUSIONS

A series of bicyclic inhibitors were prepared that employed 1-hydroxy-2-oxo-1,2-dihydro-1,8-naphthyridine-3-carboxamide (**7**) and 1,8-dihydroxy-2-oxo-1,2-dihydroquinoline-3-carboxamide (**8**) ring systems. Key features of these inhibitors include the use of a hydroxylamide group as a metal-chelating component and the inclusion of halobenzylamide functionality that is appended through a linker whose carboxamide carbonyl is not an obligatory component of the key metal-chelating heteroatom triad. Among these IN inhibitors, amides **7c** and **8c** have single digit nanomolar antiviral EC₅₀ potencies against HIV-1 vectors carrying WT IN. Several compounds have selectivity indices of greater than 20,000, and certain of these inhibitors have greater antiviral efficacies than RAL against a panel of IN mutants that included Y143R, N155H, G118R, and the double mutants G140S/Q148H and E138K/Q148K. Compounds **7c** and **8c** represent potentially useful platforms for further structural variations intended to find compounds that are more broadly effective against additional resistant strains of the virus.

EXPERIMENTAL SECTION

General Synthesis. ¹H and ¹³C NMR data were obtained on a Varian 400 MHz spectrometer or a Varian 500 MHz spectrometer and are reported in ppm relative to TMS and referenced to the solvent in which the spectra were collected. The solvent was removed by rotary evaporation under reduced pressure, and anhydrous solvents were obtained commercially and used without further drying. Purification by silica gel chromatography was performed using CombiFlash R_f 200i with EtOAc–hexanes solvent systems. Preparative high pressure liquid chromatography (HPLC) was conducted using a Waters Prep LC4000 system having photodiode array detection and Phenomenex C₁₈ columns (Cat. No. 00G-4436-P0-AX, 250 mm × 21.2 mm, 10 μm particle size, 110 Å pore) at a flow rate of 10 mL/min. Binary solvent systems consisting of A = 0.1% aqueous TFA and B = 0.1% TFA in acetonitrile were employed with gradients as indicated. Products were obtained as amorphous solids following lyophilization. Electrospray

ionization-mass spectra (ESI-MS) were acquired with an Agilent LC/MSD system equipped with a multimode ion source. Purities of samples subjected to biological testing were assessed using this system and shown to be ≥95%. High-resolution mass spectra (HRMS) were acquired by LC/MS-ESI using an LTQ-Orbitrap-XL at 30K resolution.

General Procedure A for the Synthesis of Diethyl 2-(2-(Nitrobenzylidene)malonates (10a and 10b). Commercially available 2-nitrobenzaldehydes (**9a** and **9b**) (5 mmol) were added to a solution of dimethyl malonate or diethyl malonate (60 mmol), acetic acid (20 mmol), and piperidine (6 mmol). The mixture was irradiated with microwave radiation with stirring (80 °C, 15 h). The mixture was partitioned between EtOAc (60 mL) and aqueous NaHCO₃ (30 mL), and the organic phase was dried (Na₂SO₄) and filtered, and the filtrate was concentrated. The resulting residue was purified by CombiFlash silica gel chromatography (hexanes and EtOAc) to yield either dimethyl (**10a**) or diethyl 2-(2-nitrobenzylidene)malonate (**10b**).

Dimethyl 2-(2-Nitrobenzylidene)malonate (10a). Reaction of commercially available 2-nitrobenzaldehyde (**9a**) and dimethyl malonate in benzene (8 mL) as described in general procedure A with the inclusion of benzene (8.0 mL) provided **10a** as a colorless oil in 100% yield. ¹H NMR (500 MHz, CDCl₃) δ 8.19 (t, *J* = 4.1 Hz, 2H), 7.64 (t, *J* = 7.6 Hz, 1H), 7.56 (t, *J* = 7.8 Hz, 1H), 7.39 (d, *J* = 7.6 Hz, 1H), 3.85 (s, 3H), 3.59 (s, 3H). ¹³C NMR (125 MHz, CDCl₃) δ 165.24, 163.68, 147.04, 141.73, 133.88, 130.36, 130.24, 129.92, 128.38, 125.06, 52.83, 52.42. ESI-MS *m/z*: 266.0 (M+H⁺).

Diethyl 2-(3-Methoxy-2-nitrobenzylidene)malonate (10b). Reaction of commercially available 3-methoxy-2-nitrobenzaldehyde (**9b**) and diethyl malonate as described in general procedure A, provided **10b** as a colorless oil in 90% yield. ¹H NMR (400 MHz, CDCl₃) δ 7.58 (s, 1H), 7.36 (t, *J* = 8.2 Hz, 1H), 7.05 (d, *J* = 8.4 Hz, 1H), 6.99 (d, *J* = 7.9 Hz, 1H), 4.24 (q, *J* = 7.2 Hz, 2H), 4.16 (q, *J* = 7.1 Hz, 2H), 3.87 (s, 3H), 1.27 (t, *J* = 7.1 Hz, 3H), 1.12 (t, *J* = 7.1 Hz, 3H). ¹³C NMR (100 MHz, CDCl₃) δ 164.94, 162.88, 151.25, 140.28, 135.29, 131.38 (2C), 127.75, 120.06, 114.03, 62.00, 61.73, 56.55, 13.98, 13.72. ESI-MS *m/z*: 324.1 (M+H⁺).

General Procedure B for the Synthesis of Methyl and Ethyl 1-Hydroxy-2-oxo-1,2-dihydroquinoline-3-carboxylates (11a and 11b). Compound **10a** or **10b** (0.5 mmol) was dissolved in acetic acid (3 mL) with or without added DMSO (0.8 mmol), followed by the addition of platinum(IV) oxide (0.075 mmol), and the mixture was stirred at room temperature under H₂ (22 h). The mixture was filtered and washed by MeOH, and the filtrate was concentrated and purified by CombiFlash silica gel chromatography (hexanes and EtOAc) to yield products **11a** or **11b**.

Methyl 1-Hydroxy-2-oxo-1,2-dihydroquinoline-3-carboxylate (11a). Treatment of **10a** as outlined in general procedure B, without the inclusion of DMSO, afforded **11a** as a white solid in 0.7% yield. ¹H NMR (500 MHz, CDCl₃) δ 8.63 (s, 1H), 7.80–7.77 (m, 3H), 7.39–7.36 (m, 1H), 4.01 (s, 3H). ESI-MS *m/z*: 220.0 (M+H⁺).

Ethyl 1-Hydroxy-8-methoxy-2-oxo-1,2-dihydroquinoline-3-carboxylate (11b). Treatment of **10b** as outlined in general procedure B with the inclusion of DMSO afforded **11b** as a yellow oil in 82% yield. ¹H NMR (400 MHz, CDCl₃) δ 8.47 (s, 1H), 7.31–7.29 (m, 1H), 7.23–7.22 (m, 1H), 7.21 (d, *J* = 1.6 Hz, 1H), 4.41 (q, *J* = 7.1 Hz, 2H), 3.96 (s, 3H), 1.39 (t, *J* = 7.1 Hz, 3H). ¹³C NMR (100 MHz, CDCl₃) δ 163.68, 154.45, 146.70, 141.82, 127.52, 123.81, 122.68, 119.21, 118.55, 116.62, 61.81, 57.64, 14.26. ESI-MS *m/z*: 264.1 (M+H⁺).

General Procedure C for the Synthesis of *N*-(Benzyl)-1-hydroxy-2-oxo-1,2-dihydroquinoline-3-carboxamides (12c and 13a–13c). A mixture of 11a or 11b (0.4 mmol) with benzylamine (3 mL) was heated with stirring (60 °C, 14 h), and the resulting product mixture was purified by reverse-phase HPLC to provide 12c or 13a–13c.

N-(2,4-Difluorobenzyl)-1-hydroxy-2-oxo-1,2-dihydroquinoline-3-carboxamide (12c). Treatment of 11a with 2,4-difluorobenzylamine as outlined in general procedure C with purification by preparative reverse-phase HPLC (linear gradient of 30% B to 60% B over 30 min; retention time = 28.1 min) provided 12c as a white solid. ¹H NMR (500 MHz, DMSO-*d*₆) δ 11.82 (s, 1H), 10.06 (t, *J* = 6.2 Hz, 1H), 8.84 (s, 1H), 8.05 (d, *J* = 8.0 Hz, 1H), 7.82–7.76 (m, 2H), 7.49–7.38 (m, 2H), 7.26 (t, *J* = 10.0 Hz, 1H), 7.08 (t, *J* = 8.5 Hz, 1H), 4.61 (d, *J* = 5.8 Hz, 2H). ESI-MS *m/z*: 331.1 (M+H⁺). HRMS calcd for C₁₇H₁₃F₂N₂O₃ [MH⁺], 331.0889; found, 331.0884.

N-(3-Chloro-4-fluorobenzyl)-1-hydroxy-8-methoxy-2-oxo-1,2-dihydroquinoline-3-carboxamide (13a). Reaction of 11b and 3-chloro-4-fluorobenzylamine as outlined in general procedure C with purification by preparative reverse-phase HPLC (linear gradient of 30% B to 65% B over 30 min; retention time = 27.6 min) provided 13a as a white solid in 62% yield. ¹H NMR (400 MHz, DMSO-*d*₆) δ 11.18 (s, 1H), 10.01 (t, *J* = 6.0 Hz, 1H), 8.70 (s, 1H), 7.57 (dd, *J* = 8.0, 1.2 Hz, 1H), 7.53–7.51 (m, 1H), 7.34 (ddd, *J* = 7.2, 6.8, 1.1 Hz, 3H), 7.26 (t, *J* = 7.9 Hz, 1H), 4.52 (d, *J* = 6.0 Hz, 2H), 3.83 (s, 3H). ESI-MS *m/z*: 377.0 (M+H⁺).

N-(3,4-Difluorobenzyl)-1-hydroxy-8-methoxy-2-oxo-1,2-dihydroquinoline-3-carboxamide (13b). Reaction of 11b and 3,4-difluorobenzylamine as outlined in general procedure C with purification by preparative reverse-phase HPLC (linear gradient of 30% B to 65% B over 30 min; retention time = 24.8 min) provided 13b as a white solid in 78% yield. ¹H NMR (400 MHz, DMSO-*d*₆) δ 10.08 (t, *J* = 6.0 Hz, 1H), 8.66 (s, 1H), 7.55 (dd, *J* = 8.0, 1.3 Hz, 1H), 7.38–7.21 (m, 3H), 7.17–7.14 (m, 1H), 7.12–7.08 (m, 1H), 4.51 (d, *J* = 5.9 Hz, 2H), 3.80 (s, 3H). ESI-MS *m/z*: 361.1 (M+H⁺).

N-(2,4-Difluorobenzyl)-1-hydroxy-8-methoxy-2-oxo-1,2-dihydroquinoline-3-carboxamide (13c). Reaction of 11b and 2,4-difluorobenzylamine as outlined in general procedure C with purification by preparative reverse-phase HPLC (linear gradient of 30% B to 65% B over 30 min; retention time = 27.0 min) provided 13c as a white solid in 74% yield. ¹H NMR (400 MHz, DMSO-*d*₆) δ 11.24 (s, 1H), 10.04 (t, *J* = 6.1 Hz, 1H), 8.75 (s, 1H), 7.62 (dd, *J* = 7.9, 1.3 Hz, 1H), 7.47 (dd, *J* = 15.3, 8.7 Hz, 1H), 7.42–7.40 (m, 1H), 7.32 (t, *J* = 7.9 Hz, 1H), 7.29–7.23 (m, 1H), 7.08 (dd, *J* = 11.1, 8.6 Hz, 1H), 4.59 (d, *J* = 5.9 Hz, 2H), 3.88 (s, 3H). ESI-MS *m/z*: 361.1 (M+H⁺). HRMS calcd for C₁₈H₁₅F₂N₂O₄ [MH⁺], 361.0994; found, 361.0990.

General Procedure D for the Synthesis of 1,8-Dihydroxy-2-oxo-1,2-dihydroquinoline-3-carboxamides (6a–6c). HPLC-purified compounds 13a–13c (0.1 mmol) were stirred at room temperature with boron tribromide (0.8 mmol, 2.0 M in CH₂Cl₂) (overnight). The reaction was quenched by the addition of MeOH, and the product mixture was purified by reverse-phase HPLC to provide 6a–6c.

N-(3-Chloro-4-fluorobenzyl)-1,8-dihydroxy-2-oxo-1,2-dihydroquinoline-3-carboxamide (6a). Treatment of 13a as outlined in general procedure D with purification by preparative reverse-phase HPLC (linear gradient of 30% B to 65% B over 30 min; retention time = 27.5 min) provided 6a as a white solid in 36% yield. ¹H NMR (400 MHz, DMSO-*d*₆) δ 10.14 (t, *J* = 6.0 Hz, 1H), 8.63 (s, 1H), 7.42 (dd, *J* = 7.4, 1.7 Hz, 1H), 7.39 (dd, *J* = 8.1, 1.0 Hz, 1H), 7.25–7.22 (m, 3H), 7.17 (t, *J* = 7.9 Hz, 1H), 7.06 (dd, *J* = 7.8, 1.1 Hz, 1H), 4.41 (dd, *J* = 17.7, 6.0 Hz, 2H). ESI-MS *m/z*: 363.0 (M+H⁺). HRMS calcd C₁₇H₁₃FCIN₂O₄ [MH⁺], 363.0542; found, 363.0551.

N-(3,4-Difluorobenzyl)-1,8-dihydroxy-2-oxo-1,2-dihydroquinoline-3-carboxamide (6b). Treatment of 13b as outlined in general procedure D with purification by preparative reverse-phase HPLC (linear gradient of 30% B to 65% B over 30 min; retention time = 24.9 min) provided 6b as a white solid in 42% yield. ¹H NMR (400 MHz, DMSO-*d*₆) δ 10.14 (t, *J* = 6.1 Hz, 1H), 8.63 (s, 1H), 7.39 (t, *J* = 6.4 Hz, 1H), 7.29–7.23 (m, 2H), 7.16 (t, *J* = 7.9 Hz, 2H), 7.06 (dd, *J* = 7.8, 1.2 Hz, 2H), 4.42 (dd, *J* = 24.5, 5.8 Hz, 2H). ESI-MS *m/z*: 347.1

(M+H⁺). HRMS calcd C₁₇H₁₃F₂N₂O₄ [MH⁺], 347.0838; found, 347.0847.

N-(2,4-Difluorobenzyl)-1,8-dihydroxy-2-oxo-1,2-dihydroquinoline-3-carboxamide (6c). Treatment of 13c as outlined in general procedure D with purification by preparative reverse-phase HPLC (linear gradient of 30% B to 65% B over 30 min; retention time = 24.6 min) provided 6c as a white solid in 38% yield. ¹H NMR (400 MHz, DMSO-*d*₆) δ 9.99 (t, *J* = 5.6 Hz, 1H), 8.67 (s, 1H), 7.41 (dd, *J* = 15.7, 8.0 Hz, 2H), 7.23–7.11 (m, 3H), 7.04 (dd, *J* = 19.0, 8.2 Hz, 2H), 4.54 (d, *J* = 5.9 Hz, 2H). ESI-MS *m/z*: 347.1 (M+H⁺). HRMS calcd for C₁₇H₁₃F₂N₂O₄ [MH⁺], 347.0838; found, 347.0835.

Methyl 2-(N-(Benzyloxy)-3-methoxy-3-oxopropanamido)nicotinate (15). A solution of commercially available methyl 2-fluoronicotinate (14) (1 mmol), *O*-benzylhydroxylamine (3 mmol), and *N*-ethyl-*N*-isopropylpropan-2-amine (3 mmol) in DMSO was subjected to microwave irradiation with stirring (140 °C, 10 h). The resulting mixture was extracted (EtOAc), the organic phase was washed with brine and dried (Na₂SO₄), the crude product was filtered, and the filtrate was concentrated. Purification by Combiflash silica gel chromatography (hexanes and EtOAc) provided intermediate methyl 2-((benzyloxy)amino)nicotinate as a yellow oil in 86% yield. ¹H NMR (400 MHz, CDCl₃) δ 10.03 (s, 1H), 8.49 (dd, *J* = 4.8, 1.9 Hz, 1H), 8.15 (dd, *J* = 7.8, 1.9 Hz, 1H), 7.50–7.47 (m, 2H), 7.41–7.34 (m, 3H), 6.79 (dd, *J* = 7.8, 4.8 Hz, 1H), 5.08 (s, 2H), 3.83 (s, 3H). ¹³C NMR (100 MHz, CDCl₃) δ 166.62, 159.66, 153.68 (2C), 139.85, 136.38, 128.86, 128.44, 128.26, 114.58, 114.55, 107.03, 78.05, 52.15. ESI-MS *m/z*: 259.1 (M+H⁺). To a solution of this material (2 mmol) and triethylamine (4 mmol) in CH₂Cl₂ (10 mL) was added methyl 3-chloro-3-oxopropanoate (4 mmol) dropwise, and the mixture was stirred at room temperature (2 h). The crude product was filtered, the filtrate was concentrated, and the residue was purified by Combiflash silica gel chromatography (hexanes and EtOAc) to provide 15 as a yellow oil in 83% yield. ¹H NMR (400 MHz, CDCl₃) δ 8.64 (s, 1H), 8.18 (d, *J* = 7.6 Hz, 1H), 7.39–7.38 (m, 2H), 7.35–7.32 (m, 4H), 5.03 (s, 2H), 3.88 (s, 3H), 3.72 (s, 3H), 3.61 (s, 2H). ¹³C NMR (100 MHz, CDCl₃) δ 167.09 (2C), 165.37, 151.13, 139.33, 133.89, 129.59 (3C), 128.94, 128.45 (2C), 123.83, 122.73, 78.18, 52.70, 52.32, 41.13. ESI-MS *m/z*: 359.1 (M+H⁺).

Methyl 1-(Benzyloxy)-4-hydroxy-2-oxo-1,2-dihydro-1,8-naphthyridine-3-carboxylate (16). To a solution of 15 (1.7 mmol) in MeOH (30 mL) was added sodium methanolate (4.2 mmol) (25% in MeOH) at room temperature, and the resulting suspension was stirred at room temperature (overnight). Acidification to pH 4 by the addition of aqueous 2 N HCl gave a precipitate, which was collected and dried to provide 16 as a white solid in 93% yield. ¹H NMR (400 MHz, CDCl₃) δ 8.79 (dd, *J* = 4.7, 1.8 Hz, 1H), 8.46 (dd, *J* = 7.9, 1.8 Hz, 1H), 7.73–7.71 (m, 2H), 7.41–7.36 (m, 3H), 7.28–7.25 (m, 1H), 5.28 (s, 2H), 4.08 (s, 3H). ¹³C NMR (100 MHz, CDCl₃) δ 172.35, 170.14, 156.40, 154.73, 149.54, 134.67, 134.08, 130.00 (2C), 128.94, 128.34 (2C), 118.70, 109.53, 98.85, 78.12, 53.29. ESI-MS *m/z*: 327.1 (M+H⁺).

General Procedure E for the Synthesis of 1,4-Dihydroxy-2-oxo-1,2-dihydro-1,8-naphthyridine-3-carboxamides (8a–c) and 4-Hydroxy-2-oxo-1,2-dihydro-1,8-naphthyridine-3-carboxamides (20a–20c). To a degassed solution of 16 (0.2 mmol) and MeOH (15 mL) with EtOAc (5 mL) was added Pd-C (10%, 0.2 mmol), and the mixture was stirred at room temperature under H₂ (1 h). The mixture was filtered, and the filtrate was concentrated and dissolved in DMF (1.0 mL). To this was added the appropriate halobenzylamine (2.0 mmol), and the solution was subjected to microwave irradiation with stirring (140 °C, 2 h). Purification of the reaction mixture by reverse-phase HPLC provided the desired final products 8a–c as well as the over-reduced products 20a–20c.

N-(3-Chloro-4-fluorobenzyl)-1,4-dihydroxy-2-oxo-1,2-dihydro-1,8-naphthyridine-3-carboxamide (8a) and *N*-(3-Chloro-4-fluorobenzyl)-4-hydroxy-2-oxo-1,2-dihydro-1,8-naphthyridine-3-carboxamide (20a). Treatment of 16 as outlined in general procedure E using 3-chloro-4-fluorobenzylamine with purification by preparative reverse-phase HPLC (linear gradient of 20% B to 80% B over 30 min) provided a 43% yield of 8a and 20a as white solids in a 2:1 ratio. For 8a: retention time = 26.4 min. ¹H NMR (400 MHz, DMSO-*d*₆) δ

11.01 (bs, 1H), 10.52 (bs, 1H), 8.84 (dd, $J = 4.6, 1.7$ Hz, 1H), 8.47 (dd, $J = 7.9, 1.7$ Hz, 1H), 7.60 (d, $J = 7.6$ Hz, 1H), 7.48–7.42 (m, 1H), 7.42 (d, $J = 7.7$ Hz, 2H), 4.61 (d, $J = 6.2$ Hz, 2H). ESI-MS m/z : 364.0 (M+H⁺). HRMS calcd C₁₆H₁₂ClFN₃O₄ [MH⁺], 364.0495; found, 364.0490. For **20a**: retention time = 30.7 min. ¹H NMR (400 MHz, DMSO-*d*₆) δ 12.31 (s, 1H), 10.59 (t, $J = 5.8$ Hz, 1H), 8.70 (d, $J = 4.6$ Hz, 1H), 8.36 (d, $J = 7.6$ Hz, 1H), 7.60 (d, $J = 7.0$ Hz, 1H), 7.41 (dd, $J = 9.8, 7.0$ Hz, 2H), 7.36 (dd, $J = 7.9, 4.9$ Hz, 1H), 4.59 (d, $J = 6.3$ Hz, 2H). ESI-MS m/z : 348.0 (M+H⁺). HRMS calcd C₁₆H₁₂ClFN₃O₃ [MH⁺], 348.0546; found, 348.0541.

N-(3,4-Difluorobenzyl)-1,4-dihydroxy-2-oxo-1,2-dihydro-1,8-naphthyridine-3-carboxamide (**8b**) and *N*-(3,4-Difluorobenzyl)-4-hydroxy-2-oxo-1,2-dihydro-1,8-naphthyridine-3-carboxamide (**20b**). Treatment of **16** as outlined in general procedure E using 3,4-difluorobenzylamine with purification by preparative reverse-phase HPLC (linear gradient of 20% B to 80% B over 30 min) provided a 54% yield of **8b** and **20b** as white solids in a 1:1 ratio. For **8b**: retention time = 22.2 min. ¹H NMR (400 MHz, DMSO-*d*₆) δ 11.02 (s, 1H), 10.52 (s, 1H), 8.84 (dd, $J = 4.6, 1.8$ Hz, 1H), 8.47 (dd, $J = 7.9, 1.8$ Hz, 1H), 7.51–7.37 (m, 3H), 7.24 (s, 1H), 4.60 (d, $J = 6.2$ Hz, 2H). ESI-MS m/z : 348.0 (M+H⁺). HRMS calcd C₁₆H₁₂F₂N₃O₄ [MH⁺], 348.0790; found, 348.0784. For **20b**: retention time = 27.4 min. ¹H NMR (400 MHz, DMSO-*d*₆) δ 12.33 (s, 1H), 10.59 (s, 1H), 8.70 (d, $J = 3.1$ Hz, 1H), 8.37 (d, $J = 7.8$ Hz, 1H), 7.43 (dd, $J = 14.0, 5.4$ Hz, 2H), 7.42–7.34 (m, 1H), 7.23 (bs, 1H), 4.59 (d, $J = 6.1$ Hz, 2H). ESI-MS m/z : 332.1 (M+H⁺). HRMS calcd C₁₆H₁₂F₂N₃O₃ [MH⁺], 332.0841; found, 332.0835.

N-(2,4-Difluorobenzyl)-1,4-dihydroxy-2-oxo-1,2-dihydro-1,8-naphthyridine-3-carboxamide (**8c**) and *N*-(2,4-Difluorobenzyl)-4-hydroxy-2-oxo-1,2-dihydro-1,8-naphthyridine-3-carboxamide (**20c**). Treatment of **16** as outlined in general procedure E using 2,4-difluorobenzylamine with purification by preparative reverse-phase HPLC (linear gradient of 20% B to 80% B over 30 min) provided a 45% yield of **8c** and **20c** as white solids in a 1:1 ratio. For **8c**: retention time = 24.7 min. ¹H NMR (500 MHz, DMSO-*d*₆) δ 10.95 (s, 1H), 10.42 (s, 1H), 8.77 (d, $J = 4.6$ Hz, 1H), 8.40 (d, $J = 7.9$ Hz, 1H), 7.49–7.41 (m, 1H), 7.41–7.34 (m, 1H), 7.21 (t, $J = 10.1$ Hz, 1H), 7.03 (t, $J = 8.2$ Hz, 1H), 4.57 (d, $J = 5.9$ Hz, 2H). ESI-MS m/z : 348.0 (M+H⁺). HRMS calcd C₁₆H₁₂F₂N₃O₄ [MH⁺], 348.0790; found, 348.0787. For **20c**: retention time = 29.0 min. ¹H NMR (500 MHz, DMSO-*d*₆) δ 12.32 (s, 1H), 10.57 (s, 1H), 8.70 (s, 1H), 8.36 (d, $J = 7.4$ Hz, 1H), 7.48 (d, $J = 7.5$ Hz, 1H), 7.36 (s, 1H), 7.28 (t, $J = 9.6$ Hz, 1H), 7.10 (s, 1H), 4.62 (d, $J = 5.9$ Hz, 2H). ESI-MS m/z : 332.1 (M+H⁺). HRMS calcd C₁₆H₁₂F₂N₃O₃ [MH⁺], 332.0841; found, 332.0839.

Methyl 1-(Benzyloxy)-2-oxo-4-(((trifluoromethyl)sulfonyl)oxy)-1,2-dihydro-1,8-naphthyridine-3-carboxylate (**17**). To a solution of **16** (268 mg, 0.82 mmol) and triethylamine (0.27 mL, 1.97 mmol) in CH₂Cl₂ (15 mL) was added trifluoromethanesulfonic anhydride (0.17 mL, 0.98 mmol) at 0 °C, and the solution was stirred at 0 °C (0.5 h). The mixture was concentrated and purified by Combiflash silica gel chromatography to provide **17** as a white solid (301 mg, 80% yield). ¹H NMR (400 MHz, CDCl₃) δ 8.86 (dd, $J = 4.7, 1.7$ Hz, 1H), 8.21 (dd, $J = 8.1, 1.7$ Hz, 1H), 7.70–7.67 (m, 2H), 7.43–7.38 (m, 4H), 5.34 (s, 2H), 4.01 (s, 3H). ¹³C NMR (100 MHz, CDCl₃) δ 160.87, 155.20, 154.02, 153.98, 148.70, 148.09, 133.32, 133.23, 130.12, 129.33, 128.48, 120.84, 119.91, 119.86, 116.67, 109.73, 78.72, 53.50. ESI-MS m/z : 459.0 (M+H⁺).

Methyl 1-(Benzyloxy)-2-oxo-1,2-dihydro-1,8-naphthyridine-3-carboxylate (**18**). To a mixture of **17** (34 mg, 0.074 mmol) and PdCl₂(PPh₃)₂ (5 mg, 7.37 μ mol) in DMF (1 mL), triethylamine (0.030 mL, 0.22 mmol) and triisopropylsilane (17 mg, 0.15 mmol) were added. The mixture was heated to 85 °C (24 h). The resulting crude mixture was purified by Combiflash silica gel chromatography (hexanes and EtOAc) to provide **18** as a white solid (12 mg, 52% yield). ¹H NMR (400 MHz, CDCl₃) δ 8.74 (dd, $J = 4.7, 1.8$ Hz, 1H), 8.41 (s, 1H), 7.99 (dd, $J = 7.8, 1.7$ Hz, 1H), 7.69 (dd, $J = 7.6, 1.8$ Hz, 2H), 7.38–7.30 (m, 3H), 7.26–7.23 (m, 1H), 5.29 (s, 2H), 3.96 (s, 3H). ¹³C NMR (100 MHz, CDCl₃) δ 164.47, 153.41, 141.78, 138.27, 133.86, 132.08, 131.99, 130.10 (2C), 129.05, 128.50, 128.37 (2C), 119.32, 113.30, 78.21, 52.90. ESI-MS m/z : 311.1 (M+H⁺).

General Procedure F for the Synthesis of 1-(Benzyloxy)-*N*-(halobenzyl)-2-oxo-1,2-dihydro-1,8-naphthyridine-3-carboxamides (19a–19c). A solution of **18** (0.6 mmol) and halobenzylamine (1 mL) was heated with stirring (60 °C, 14 h). The mixture was then extracted (CHCl₃) and washed sequentially with aqueous 1 N HCl and brine and dried (Na₂SO₄). The organic phase was filtered and concentrated, and the crude residue was purified by Combiflash silica gel chromatography (hexanes and EtOAc) to provide amides **19(a–c)**.

1-(Benzyloxy)-*N*-(3-chloro-4-fluorobenzyl)-2-oxo-1,2-dihydro-1,8-naphthyridine-3-carboxamide (**19a**). Treatment of **18** with 3-chloro-4-difluorobenzylamine as outlined in general procedure F provided **19a** as a white solid in 31% yield. ¹H NMR (400 MHz, CDCl₃) δ 9.90 (t, $J = 5.7$ Hz, 1H), 8.81 (s, 1H), 8.75 (dd, $J = 4.7, 1.8$ Hz, 1H), 8.06 (dd, $J = 7.8, 1.8$ Hz, 1H), 7.61–7.60 (m, 1H), 7.59 (d, $J = 1.7$ Hz, 1H), 7.36–7.32 (m, 2H), 7.31–7.27 (m, 3H), 7.19–7.15 (m, 1H), 7.03 (t, $J = 8.7$ Hz, 1H), 5.27 (s, 2H), 4.56 (d, $J = 6.0$ Hz, 2H). ¹³C NMR (100 MHz, CDCl₃) δ 162.45, 159.38, 157.35 (d, $J = 248.3$ Hz), 153.33, 148.97, 141.41, 138.72, 135.31 (d, $J = 3.9$ Hz), 133.56, 129.94 (2C), 129.87, 129.24, 128.49 (2C), 128.38 (d, $J = 15.3$ Hz), 127.43 (d, $J = 7.3$ Hz), 123.36, 120.00, 116.61 (d, $J = 21.2$ Hz), 114.12, 78.57, 42.58. ESI-MS m/z : 438.1 (M+H⁺).

1-(Benzyloxy)-*N*-(3,4-difluorobenzyl)-2-oxo-1,2-dihydro-1,8-naphthyridine-3-carboxamide (**19b**). Treatment of **18** with 3,4-difluorobenzylamine as outlined in general procedure F provided **19b** as a white solid in 51% yield. ¹H NMR (400 MHz, CDCl₃) δ 9.95 (t, $J = 5.8$ Hz, 1H), 8.85 (s, 1H), 8.78 (dd, $J = 4.7, 1.8$ Hz, 1H), 8.09 (dd, $J = 7.8, 1.7$ Hz, 1H), 7.65–7.64 (m, 1H), 7.62 (d, $J = 1.7$ Hz, 1H), 7.37–7.30 (m, 4H), 7.20–7.13 (m, 1H), 7.09–7.03 (m, 1H), 6.98–6.94 (m, 1H), 5.29 (s, 2H), 4.59 (d, $J = 6.0$ Hz, 2H). ESI-MS m/z : 422.1 (M+H⁺).

1-(Benzyloxy)-*N*-(2,4-difluorobenzyl)-2-oxo-1,2-dihydro-1,8-naphthyridine-3-carboxamide (**19c**). Treatment of **18** with 2,4-difluorobenzylamine as outlined in general procedure F provided **19c** as a white solid in 22% yield. ¹H NMR (400 MHz, CDCl₃) δ 9.92 (d, $J = 5.4$ Hz, 1H), 8.87 (s, 1H), 8.82 (ddd, $J = 4.7, 1.7, 0.6$ Hz, 1H), 8.13 (dd, $J = 7.8, 1.7$ Hz, 1H), 7.69 (d, $J = 2.4$ Hz, 1H), 7.68 (dd, $J = 3.3, 1.3$ Hz, 1H), 7.42–7.34 (m, 5H), 6.88–6.76 (m, 2H), 5.34 (s, 2H), 4.69 (d, $J = 5.9$ Hz, 2H). ESI-MS m/z : 422.1 (M+H⁺).

General Procedure G for the Synthesis of 1-(Benzyloxy)-*N*-(halobenzyl)-2-oxo-1,2-dihydro-1,8-naphthyridine-3-carboxamides 7(a–c). To a solution of amide (**19a–19c**) (0.2 mmol) in a solution of MeOH (10 mL) and EtOAc (3 mL) was added Pd-C (10%, 20 mg), and the mixture was degassed and stirred at room temperature under H₂ (1 h). The mixture was then filtered through a small pad of silica gel, the filtrate was concentrated, and the residue was purified by preparative reverse-phase HPLC to provide the target amides **7a–c**.

N-(3-Chloro-4-fluorobenzyl)-1-hydroxy-2-oxo-1,2-dihydro-1,8-naphthyridine-3-carboxamide (**7a**). Treatment of **19a** as outlined in general procedure G and purification by preparative reverse-phase HPLC (linear gradient of 30% B to 50% B over 30 min; retention time = 22.5 min) provided **7a** as a white solid in 41% yield. ¹H NMR (400 MHz, DMSO-*d*₆) δ 11.42 (bs, 1H), 9.96 (t, $J = 5.9$ Hz, 1H), 8.85 (s, 1H), 8.82 (dd, $J = 4.7, 1.8$ Hz, 1H), 8.51 (dd, $J = 7.9, 1.8$ Hz, 1H), 7.58 (d, $J = 7.8$ Hz, 1H), 7.47 (dd, $J = 7.8, 4.7$ Hz, 1H), 7.40–7.37 (m, 2H), 4.58 (d, $J = 6.0$ Hz, 2H). ESI-MS m/z : 348.0 (M+H⁺). HRMS calcd C₁₆H₁₂ClFN₃O₃ [MH⁺], 348.0546; found, 348.0542.

N-(3,4-Difluorobenzyl)-1-hydroxy-2-oxo-1,2-dihydro-1,8-naphthyridine-3-carboxamide (**7b**). Treatment of **19b** as outlined in general procedure G and purification by preparative reverse-phase HPLC (linear gradient of 20% B to 50% B over 30 min; retention time = 26.1 min) provided **7b** as a white solid in 22% yield. ¹H NMR (400 MHz, DMSO-*d*₆) δ 11.42 (bs, 1H), 9.96 (t, $J = 6.0$ Hz, 1H), 8.85 (s, 1H), 8.82 (dd, $J = 4.7, 1.8$ Hz, 1H), 8.52 (dd, $J = 7.8, 1.8$ Hz, 1H), 7.47 (dd, $J = 7.8, 4.7$ Hz, 1H), 7.45–7.37 (m, 2H), 7.23–7.22 (m, 1H), 4.58 (d, $J = 6.1$ Hz, 2H). ESI-MS m/z : 332.1 (M+H⁺). HRMS calcd C₁₈H₁₂F₂N₃O₃ [MH⁺], 332.0841; found, 332.0828.

N-(2,4-Difluorobenzyl)-1-hydroxy-2-oxo-1,2-dihydro-1,8-naphthyridine-3-carboxamide (**7c**). Treatment of **19c** as outlined in general procedure G and purification by preparative reverse-phase HPLC (linear gradient of 20% B to 80% B over 30 min; retention time

= 19.2 min) provided **7c** as a white solid in 52% yield. $^1\text{H NMR}$ (400 MHz, $\text{DMSO-}d_6$) δ 9.88 (t, $J = 5.9$ Hz, 1H), 8.78 (s, 1H), 8.75 (dd, $J = 4.7, 1.8$ Hz, 1H), 8.45 (dd, $J = 7.9, 1.8$ Hz, 1H), 7.46–7.34 (m, 2H), 7.19 (ddd, $J = 10.6, 9.4, 2.6$ Hz, 1H), 7.03–6.98 (m, 1H), 4.54 (d, $J = 5.9$ Hz, 2H). ESI-MS m/z : 332.1 ($\text{M}+\text{H}^+$). HRMS calcd $\text{C}_{16}\text{H}_{12}\text{F}_2\text{N}_3\text{O}_3$ [MH^+], 332.0841; found, 332.0834.

Integrase Assays. IN reactions were performed as previously described.³⁵ Briefly, reactions were carried out by adding compounds or an equivalent volume of 100% DMSO (used as solvent for the compounds) to a mixture of 20 nM [γ - ^{32}P]-labeled DNA and 400 nM IN in a buffer containing 50 mM morpholinepropanesulfonic acid (pH 7.2), 7.5 mM MgCl_2 , and 14 mM 2-mercaptoethanol. [γ - ^{32}P]-labeled full length oligonucleotide 21T (GTGTGGAAAATCTCTAGCAGT) or precleaved oligonucleotide 19T (GTGTGGAAAATCTCTAGCA), both annealed to the complementary oligonucleotide 21B (ACTGCTAGAGATTTTCCACAC), were used to measure both 3'-processing and strand transfer, respectively.³⁵ Reactions were performed at 37 °C for 2 h and quenched by the addition of an equal volume of loading buffer (formamide containing 1% sodium dodecyl sulfate, 0.25% bromophenol blue, and xylene cyanol). Reaction products were separated in 16% polyacrylamide-denaturing sequencing gels. Dried gels were visualized using Typhoon 8600 (GE Healthcare, Piscataway, NJ). Densitometric analyses were performed using ImageQuant 5.1 software from GE Healthcare. The data analyses (linear regression, 50% inhibitory concentration [IC_{50}] determination, and standard deviation [SD]) were performed from at least 3 independent determinations using Prism 5.0c software from GraphPad.

Cellular Cytotoxicity Assays. The human osteosarcoma cell line, HOS, was obtained from Dr. Richard Schwartz (Michigan State University, East Lansing, MI) and grown in Dulbecco's modified Eagle's medium (Invitrogen, Carlsbad, CA) supplemented with 5% (v/v) fetal bovine serum, 5% newborn calf serum, and penicillin (50 units/mL) plus streptomycin (50 $\mu\text{g}/\text{mL}$; Quality Biological, Gaithersburg, MD). On the day prior to the screen, HOS cells were seeded in a 96-well luminescence cell culture plate at a density of 4000 cells in 100 μL per well. On the day of the screen, cells were treated with compounds in the appropriate concentration range chosen and incubated at 37 °C for 48 h. Cytotoxicity was measured by monitoring ATP levels via a luciferase reporter assay. Cells were lysed in 50 μL of cell lysis buffer (PerkinElmer, Waltham, MA) and shaken at 700 rpm at room temperature for 5 min. After the addition of 50 μL of ATPlite buffer (PerkinElmer) directly onto the lysed cells and shaking at 700 rpm at room temperature (5 min), ATP levels were monitored by measuring luciferase activity using a microplate reader. Activity was normalized to cytotoxicity in the absence of target compounds. KaleidaGraph (Synergy Software, Reading, PA) was used to perform regression analysis on the data. CC_{50} values were determined from the fit model.

Single-Round HIV-1 Infectivity Assays. Human embryonic kidney cell line 293T was transfected with the pNLN_{go}MIVR- Δ LUC vector, which was made from pNLN_{go}MIVR- Δ Env-HSA by removing the HSA reporter gene and replacing it with a luciferase reporter gene between the NotI and XhoI restriction sites.³⁷ VSV-g-pseudotyped HIV was produced by transfections of 293T cells as described previously.³⁸ On the day prior to transfection, 293T cells were plated on 100-mm-diameter dishes at a density of 1.5×10^6 cells per plate. 293T cells were transfected with 16 μg of pNLN_{go}MIVR- Δ LUC and 4 μg of pHCMV-g (obtained from Dr. Jane Burns, University of California, San Diego) using the calcium phosphate method. At approximately 6 h after the calcium phosphate precipitate was added, the 293T cells were washed twice with phosphate-buffered saline (PBS) and incubated with fresh media (48 h). The virus-containing supernatants were then harvested, clarified by low-speed centrifugation, filtered, and diluted for preparation in infection assays. On the day prior to the screen, HOS cells were seeded in a 96-well luminescence cell culture plate at a density of 4000 cells in 100 μL per well. On the day of the screen, cells were treated with the compounds from a concentration range of 10 μM to 0.0005 μM using 11 serial dilutions and then incubated at 37 °C (3 h). After this incubation, 100 μL of virus-stock diluted to achieve a maximum luciferase signal

between 0.2 and 1.5 RLU was added to each well, and the plates were incubated at 37 °C (48 h). Infectivity was measured by using the Steady-lite plus luminescence reporter gene assay system (PerkinElmer, Waltham, MA). Luciferase activity was measured by adding 100 μL of Steady-lite plus buffer (PerkinElmer) to the cells, incubating at room temperature (20 min), and measuring luminescence using a microplate reader. Activity was normalized to infectivity in the absence of target compounds. KaleidaGraph (Synergy Software, Reading, PA) was used to perform regression analysis on the data. EC_{50} values were determined from the fit model.

Vector Constructs. pNLN_{go}MIVR- Δ Env-LUC has been described previously.³⁷ The IN coding region was removed from pNLN_{go}MIVR- Δ Env-LUC (between *KpnI* and *Sall* sites) and inserted between the *KpnI* and *Sall* sites of pBluescript II KS+. Using that construct as the wild-type template, we prepared the following IN-resistant mutants via the QuikChange II XL (Stratagene, La Jolla, CA) site-directed mutagenesis protocol: G118R, Y143R, Q148H, Q148K, N155H, G140S + Q148H, G140A + Q148K, and E138K + Q148K. The following sense with cognate antisense (not shown) oligonucleotides (Integrated DNA Technologies, Coralville, IA) was used in the mutagenesis: G118R, 5'-GTACATACAGACAATCGCAGCAATTTCCACCAGTAC-3'; E138K, 5'-GGCGGGATCAAGCAGAAAATTTGGCATTCCCTA-3'; G140A, 5'-GGGGATCAAGCAGGAATTTGCCATTCCCTACAATC-3'; G140S, 5'-GGGGATCAAGCAGGAATTTAGCATTCCCTACAATC-3'; Y143R, 5'-GCAGGAATTTGGCATTCCCCGC-AATCCCCAAAGTCAAGGA-3'; Q148H, 5'-CATTCCCTACAA-TCCCCAAAGTCATGGAGTAATAGAATCTA-3'; Q148K, 5'-CATTCCCTACAATCCCCAAAGTAAAGGAGTAATAGAATCTATGAA-3'; and N155H, 5'-CCAAAGTCAAGGAGTAATAGAATCTATGCATAAAGAATTAAGAAAATTATAGGACA-3'. The double mutant G140S + Q148H was constructed by using the previously generated Q148H mutant and the appropriate oligonucleotide to introduce the second mutation, G140S. The double mutant G140A + Q148K was made by using the Q148K mutant and the appropriate oligonucleotide to introduce the second mutation, G140A. The double mutant E138K + Q148K was made by using the Q148K mutant and the appropriate oligonucleotide to introduce the second mutation, E138K. The DNA sequence of each construct was verified independently by DNA sequencing. The mutant IN coding sequences from pBluescript II KS+ were then subcloned into pNLN_{go}MIVR- Δ Env-LUC (between the *KpnI* and *Sall* sites) to produce the full-length mutant HIV-1 IN constructs. These DNA sequences were additionally checked independently by DNA sequencing.

AUTHOR INFORMATION

Corresponding Author

*Tel: 301-846-5906. Fax: 301-846-6033. E-mail: burkete@helix.nih.gov.

Present Address

^{||}Laboratoire MFP, CNRS - UMR 5234, Université de Bordeaux, Bordeaux Cedex 33076, France

Notes

The content of this publication does not necessarily reflect the views or policies of the Department of Health and Human Services, nor does mention of trade names, commercial products, or organizations imply endorsement by the U.S. Government.

The authors declare no competing financial interest.

ACKNOWLEDGMENTS

This work was supported in part by the Intramural Research Program of the NIH, Center for Cancer Research, Frederick National Laboratory for Cancer Research and the National Cancer Institute, National Institutes of Health and the Joint Science and Technology Office of the Department of Defense,

and by funds from the Intramural AIDS Targeted Antiviral Program.

■ ABBREVIATIONS USED

HIV-1, human immunodeficiency virus type 1; AIDS, acquired immune deficiency syndrome; FDA, Food and Drug Administration; IN, integrase; RAL, Raltegravir; EVG, Elvitegravir; DTG, Dolutegravir; 3'-P, 3'-processing; ST, strand transfer; INSTIs, integrase strand transfer inhibitors; DNA, deoxyribonucleic acid; IC₅₀, half-maximum inhibitory concentration; EC₅₀, half maximal effective concentration; WT, wild type; DMSO, dimethyl sulfoxide; DMF, dimethylformamide; HPLC, high-pressure liquid chromatography; HRMS, high-resolution mass spectrometry

■ REFERENCES

- (1) Metifiot, M.; Marchand, C.; Pommier, Y. HIV integrase inhibitors: 20-Year landmark and challenges. *Adv. Pharmacol.* **2013**, *67*, 75–105.
- (2) Di Santo, R. Inhibiting the HIV integration process: past, present, and the future. *J. Med. Chem.* **2013**, DOI: 10.1021/jm400674a.
- (3) Croxtall, J. D.; Scott, L. J. Raltegravir: In treatment-naive patients with HIV-1 infection. *Drugs* **2010**, *70*, 631–642.
- (4) Wills, T.; Vega, V. Elvitegravir: A once-daily inhibitor of HIV-1 integrase. *Expert Opin. Invest. Drugs* **2012**, *21*, 395–401.
- (5) Marchand, C.; Maddali, K.; Metifiot, M.; Pommier, Y. HIV-1 IN inhibitors: 2010 Update and perspectives. *Curr. Top. Med. Chem.* **2009**, *9*, 1016–1037.
- (6) Metifiot, M.; Marchand, C.; Maddali, K.; Pommier, Y. Resistance to integrase inhibitors. *Viruses* **2010**, *2*, 1347–1366.
- (7) Cherepanov, P.; Maertens, G. N.; Hare, S. Structural insights into the retroviral DNA integration apparatus. *Curr. Opin. Struct. Biol.* **2011**, *21*, 249–256.
- (8) Perryman, A. L.; Forli, S.; Morris, G. M.; Burt, C.; Cheng, Y.; Palmer, M. J.; Whitby, K.; McCammon, J. A.; Phillips, C.; Olson, A. J. A dynamic model of HIV integrase inhibition and drug resistance. *J. Mol. Biol.* **2010**, *397*, 600–615.
- (9) Geretti, A. M.; Armenia, D.; Ceccherini-Silberstein, F. Emerging patterns and implications of HIV-1 integrase inhibitor resistance. *Curr. Opin. Infect. Dis.* **2012**, *25*, 677–686.
- (10) Delelis, O.; Thierry, S.; Subra, F.; Simon, F.; Malet, I.; Alloui, C.; Sayon, S.; Calvez, V.; Deprez, E.; Marcelin, A.-G.; Tchertanov, L.; Mouscadet, J.-F. Impact of Y143 HIV-1 integrase mutations on resistance to raltegravir in vitro and in vivo. *Antimicrob. Agents Chemother.* **2009**, *54*, 491–501.
- (11) Quashie, P. K.; Sloan, R. D.; Wainberg, M. A. Novel therapeutic strategies targeting HIV integrase. *BMC Med.* **2012**, *10* (34), DOI: 10.1186/1741-7015-10-34.
- (12) Katlama, C.; Murphy, R. Dolutegravir for the treatment of HIV. *Expert Opin. Invest. Drugs* **2012**, *21*, 523–530.
- (13) Ballantyne, A. D.; Perry, C. M. Dolutegravir: first global approval. *Drugs* **2013**, *73*, 1627–1637.
- (14) Vandekerckhove, L. GSK-1349572, a novel integrase inhibitor for the treatment of HIV infection. *Curr. Opin. Invest. Drugs* **2010**, *11*, 203–212.
- (15) Kawasuji, T.; Johns, B. A.; Yoshida, H.; Taishi, T.; Taoda, Y.; Murai, H.; Kiyama, R.; Fuji, M.; Yoshinaga, T.; Seki, T.; Kobayashi, M.; Sato, A.; Fujiwara, T. Carbamoyl pyridone HIV-1 integrase inhibitors. 1. Molecular design and establishment of an advanced two-metal binding pharmacophore. *J. Med. Chem.* **2012**, *55*, 8735–8744.
- (16) Kawasuji, T.; Johns, B. A.; Yoshida, H.; Weatherhead, J. G.; Akiyama, T.; Taishi, T.; Taoda, Y.; Mikamiyama-Iwata, M.; Murai, H.; Kiyama, R.; Fuji, M.; Tanimoto, N.; Yoshinaga, T.; Seki, T.; Kobayashi, M.; Sato, A.; Garvey, E. P.; Fujiwara, T. Carbamoyl pyridone HIV-1 integrase inhibitors. 2. Bi- and tricyclic derivatives result in superior antiviral and pharmacokinetic profiles. *J. Med. Chem.* **2013**, *56*, 1124–1135.
- (17) Johns, B. A.; Kawasuji, T.; Weatherhead, J. G.; Taishi, T.; Temelkoff, D. P.; Yoshida, H.; Akiyama, T.; Taoda, Y.; Murai, H.; Kiyama, R.; Fuji, M.; Tanimoto, N.; Jeffrey, J.; Foster, S. A.; Yoshinaga, T.; Seki, T.; Kobayashi, M.; Sato, A.; Johnson, M. N.; Garvey, E. P.; Fujiwara, T. Carbamoyl pyridone HIV-1 integrase inhibitors 3. A diastereomeric approach to chiral nonracemic tricyclic ring systems and the discovery of dolutegravir (S/GSK1349572) and (S/GSK1265744). *J. Med. Chem.* **2013**, *56*, 5901–5916.
- (18) Metifiot, M.; Maddali, K.; Johnson, B. C.; Hare, S.; Smith, S. J.; Zhao, X. Z.; Marchand, C.; Burke, T. R., Jr.; Hughes, S. H.; Cherepanov, P.; Pommier, Y. Activities, crystal structures and molecular dynamics of dihydro-1*H*-isoindole derivatives, inhibitors of HIV-1 integrase. *ACS Chem. Biol.* **2013**, *8*, 209–217.
- (19) Sangeetha, B.; Muthukumar, R.; Amutha, R. Pharmacophore modelling and electronic feature analysis of hydroxamic acid derivatives, the HIV integrase inhibitors. *SAR QSAR Environ. Res.* **2013**, *24*, 753–771.
- (20) Plewe, M. B.; Butler, S. L.; R, D. K.; Hu, Q.; Johnson, T. W.; Kuehler, J. E.; Kuki, A.; Lam, H.; Liu, W.; Nowlin, D.; Peng, Q.; Rahavendran, S. V.; Tanis, S. P.; Tran, K. T.; Wang, H.; Yang, A.; Zhang, J. Azaindole hydroxamic acids are potent HIV-1 integrase inhibitors. *J. Med. Chem.* **2009**, *52*, 7211–7219.
- (21) Tang, J.; Maddali, K.; Metifiot, M.; Sham Yuk, Y.; Vince, R.; Pommier, Y.; Wang, Z. 3-Hydroxypyrimidine-2,4-diones as an inhibitor scaffold of HIV integrase. *J. Med. Chem.* **2011**, *54*, 2282–2292.
- (22) Johnson, T. W.; Tanis, S. P.; Butler, S. L.; Dalvie, D.; DeLisle, D. M.; Dress, K. R.; Flahive, E. J.; Hu, Q.; Kuehler, J. E.; Kuki, A.; Liu, W.; McClellan, G. A.; Peng, Q.; Plewe, M. B.; Richardson, P. F.; Smith, G. L.; Solowiej, J.; Tran, K. T.; Wang, H.; Yu, X.; Zhang, J.; Zhu, H. Design and synthesis of novel *N*-hydroxy-dihydronaphthyridinones as potent and orally bioavailable HIV-1 integrase inhibitors. *J. Med. Chem.* **2011**, *54*, 3393–3417.
- (23) Desimmie, B. A.; Demeulemeester, J.; Suchaud, V.; Taltynov, O.; Billamboz, M.; Lion, C.; Bailly, F.; Strelkov, S.; Debyser, Z.; Cotellet, P.; Christ, F. 2-Hydroxyisoquinoline-1,3(2*H*,4*H*)-diones (HIDs), novel inhibitors of HIV integrase with a high barrier to resistance. *ACS Chem. Biol.* **2013**, *8*, 1187–1194.
- (24) Billamboz, M.; Suchaud, V.; Bailly, F.; Lion, C.; Demeulemeester, J.; Calmels, C.; Andreola, M.-L.; Christ, F.; Debyser, Z.; Cotellet, P. 4-Substituted 2-hydroxyisoquinoline-1,3(2*H*,4*H*)-diones as a novel class of HIV-1 integrase inhibitors. *ACS Med. Chem. Lett.* **2013**, *4*, 606–611.
- (25) Pryde, D. C.; Webster, R.; Butler, S. L.; Murray, E. J.; Whitby, K.; Pickford, C.; Westby, M.; Palmer, M. J.; Bull, D. J.; Vuong, H.; Blakemore, D. C.; Stead, D.; Ashcroft, C.; Gardner, I.; Bru, C.; Cheung, W.-Y.; Roberts, I. O.; Morton, J.; Bissell, R. A. Discovery of an HIV integrase inhibitor with an excellent resistance profile. *MedChemComm* **2013**, *4*, 709–719.
- (26) Zhao, X. Z.; Maddali, K.; Vu, B. C.; Marchand, C.; Hughes Stephen, H.; Pommier, Y.; Burke Terrence, R., Jr. Examination of halogen substituent effects on HIV-1 integrase inhibitors derived from 2,3-dihydro-6,7-dihydroxy-1*H*-isoindol-1-ones and 4,5-dihydroxy-1*H*-isoindole-1,3(2*H*)-diones. *Bioorg. Med. Chem. Lett.* **2009**, *19*, 2714–2717.
- (27) Flipo, M.; Beghyn, T.; Leroux, V.; Florent, I.; Deprez, B. P.; Deprez-Poulain, R. F. Novel selective inhibitors of the zinc plasmodial aminopeptidase PfA-M1 as potential antimalarial agents. *J. Med. Chem.* **2007**, *50*, 1322–1334.
- (28) Nicolau, K. C.; Xu, J. Y.; Kim, S.; Ohshima, T.; Hosokawa, S.; Pfeifferkorn, J. Synthesis of the tricyclic core of eleutherobin and sarcodictyins and total synthesis of sarcodictyin A. *J. Am. Chem. Soc.* **1997**, *119*, 11353–11354.
- (29) Rylander, P. N.; Karpenko, I. M.; Pond, G. R. Selectivity of hydrogenation over platinum metal catalysts: nitroaromatics. *Ann. N.Y. Acad. Sci.* **1970**, *172*, 266–275.
- (30) Takenaka, Y.; Kiyosu, T.; Choi, J.-C.; Sakakura, T.; Yasuda, H. Selective synthesis of *N*-aryl hydroxylamines by the hydrogenation of

nitroaromatics using supported platinum catalysts. *Green Chem.* **2009**, *11*, 1385–1390.

(31) Zhao, X. Z.; Maddali, K.; Smith, S. J.; Metifiot, M.; Johnson, B.; Hughes, S. H.; Pommier, Y.; Burke, T. R., Jr. 6,7-Dihydroxy-1-oxoisindoline-4-sulfonamide-containing HIV-1 Integrase Inhibitors. *Bioorg. Med. Chem. Lett.* **2012**, *22*, 7309–7313.

(32) Williams, P. D.; Venkatraman, S.; Langford, H. M.; Kim, B.; Booth, T. M.; Grobler, J. A.; Staas, D.; Ruzek, R. D.; Embrey, M. W.; Wiscount, C. M.; Lyle, T. A. Preparation of 1-Hydroxynaphthyridin-2(1H)-one Derivatives as Anti-HIV Agents. Patent WO2008010964(A1).

(33) Zhao, X. Z.; Semenova, E. A.; Vu, B. C.; Maddali, K.; Marchand, C.; Hughes, S. H.; Pommier, Y.; Burke, T. R., Jr. 2,3-Dihydro-6,7-dihydroxy-1H-isindol-1-one-based HIV-1 integrase inhibitors. *J. Med. Chem.* **2008**, *51*, 251–259.

(34) Malet, I.; Delelis, O.; Valantin, M.-A.; Montes, B.; Soulie, C.; Wiriden, M.; Tchertanov, L.; Peytavin, G.; Reynes, J.; Mouscadet, J.-F.; Katlama, C.; Calvez, V.; Marcelin, A.-G. Mutations associated with failure of raltegravir treatment affect integrase sensitivity to the inhibitor in vitro. *Antimicrob. Agents Chemother.* **2008**, *52*, 1351–1358.

(35) Metifiot, M.; Maddali, K.; Naumova, A.; Zhang, X.; Marchand, C.; Pommier, Y. Biochemical and pharmacological analyses of HIV-1 integrase flexible loop mutants resistant to raltegravir. *Biochemistry* **2010**, *49*, 3715–3722.

(36) Mesplede, T.; Quashie, P. K.; Wainberg, M. A. Resistance to HIV integrase inhibitors. *Curr. Opin. HIV AIDS* **2012**, *7*, 401–408.

(37) Zhao, X. Z.; Maddali, K.; Metifiot, M.; Smith, S. J.; Vu, B. C.; Marchand, C.; Hughes, S. H.; Pommier, Y.; Burke, T. R., Jr. Bicyclic hydroxy-1H-pyrrolopyridine-trione containing HIV-1 integrase inhibitors. *Chem. Biol. Drug Des.* **2012**, *79*, 157–165.

(38) Brachmann, A.; Koenig, J.; Julius, C.; Feldbruegge, M. A reverse genetic approach for generating gene replacement mutants in *Ustilago maydis*. *Mol. Genet. Genomics* **2004**, *272*, 216–226.